J. Fluid Mech. (2010), *vol.* 647, *pp.* 335–359.
doi:10.1017/S0022112010000108

Instability of uniform micro-organism suspensions revisited

T. J. PEDLEY†

Department of Applied Mathematics and Theoretical Physics, CMS, Wilberforce Road, Cambridge CB3 0WA, UK

(Received 13 October 2009; revised 21 December 2009; accepted 28 December 2009)

Uniform suspensions of bottom-heavy, upswimming (gyrotactic) micro-organisms that are denser than water are unstable, through a gravitational mechanism first described by Pedley, Hill & Kessler (*J. Fluid Mech.*, vol. 195, 1988, p. 223). Suspensions of downswimming, head-heavy cells do not experience this instability. In the absence of gravity, a uniform suspension of swimming micro-organisms may be unstable because of the 'particle stresses' generated by the swimming cells themselves, each of which acts as a force-dipole or stresslet (Simha & Ramaswamy, *Phys. Rev. Lett.*, vol. 89, 2002, p. 058101). The stresslet strength S is positive for 'pullers' such as algae and negative for 'pushers' such as bacteria or spermatozoa. In this paper, the combined problem is investigated, with attention being paid also to the effect of rotational diffusivity and to whether the probability density function $f(\boldsymbol{e})$ for the cells' swimming direction $\boldsymbol{e}$ can be approximated as quasi-steady in calculations of the mean swimming direction, which arises in the cell conservation equation, and the particle stress tensor, which appears in the momentum equation. The existence of both the previous instabilities is confirmed at long wavelength. However, the non-quasi-steadiness of the orientation distribution means that the particle-stress-driven instability no longer arises for arbitrarily small $|S|$, in the Stokes limit, but requires that the dimensionless stresslet strength (proportional to the product of S and the basic state cell volume fraction n_o) exceed a critical value involving both viscosity and rotational diffusivity. In addition, a new mode of gravitational instability is found for 'head-heavy' cells, even when they exert no particle stresses ($S = 0$), in the form of weakly growing waves. This is a consequence of unsteadiness in the mean swimming direction, together with non-zero fluid inertia. For realistic parameter values, however, viscosity is expected to suppress this instability.

1. Introduction

Bioconvection is the name given to the pattern-forming motions that arise in a shallow suspension of upswimming micro-organisms that are denser than the suspending fluid. The cells tend to accumulate near the upper surface of the suspension, generating a density stratification that is gravitationally unstable, and which leads to convection in the suspension as a whole. Rational fluid dynamic modelling of bioconvection was initiated by Childress, Levandowsky & Spiegel (1975), who assumed that individual cells always swim vertically upwards relative to the fluid. Kessler (1984, 1985, 1986) hypothesized and then demonstrated that certain algal cells

† Email address for correspondence: t.j.pedley@damtp.cam.ac.uk

swim upwards on average because they are bottom-heavy, i.e. the centre of mass lies behind the centre of buoyancy, so that a cell that is not oriented vertically will experience a gravitational torque tending to restore it to the vertical. However, when suspended in a moving fluid, a cell will also experience a viscous torque, related to the velocity gradient in the flow, and will swim in a direction determined by the balance of viscous and gravitational torques. In particular, in a vertical shear flow (e.g. downflow in a vertical pipe) cells will tend to swim towards the region(s) of most rapid downflow, such as the pipe axis (Kessler 1985).

If cells were front- or head-heavy, a similar mechanism would cause cells to swim downwards in still fluid, and towards the region(s) of most rapid upflow, or slowest downflow, in a vertical shear flow. A similar effect can be achieved by cells of homogeneous density greater than that of water if their geometry is asymmetric. Consider a spermatozoon or a bacterium, for example, with a long slender flagellum (or flagellar bundle) at the rear of a compact head, and suppose that it is released from rest in a horizontal orientation. It will sink, because it is denser than the fluid, but will also rotate because the centre of mass is located in or near the head, and the viscous torque on the tail outweighs that on the head. Thus, it will naturally develop a head-down orientation, just as if it were head-heavy (Katz & Pedrotti 1977; Roberts & Deacon 2002), and will respond to shear in the same way.

The above orientation mechanism, termed 'gyrotaxis', leads to a mechanism for instability of a uniform suspension of bottom-heavy cells, without density stratification. Suppose that natural fluctuations cause a 'blob' of fluid to contain more cells per unit volume than its neighbours. This blob will sink relative to its surroundings, thereby generating a downwards shear flow, with maximum velocity in the blob. The gyrotactic torque balance will then cause other cells to swim in towards the blob or its wake, reinforcing the density difference and speeding up the downflow. This mechanism would not operate for head-heavy cells, for which gyrotaxis would be stabilizing. Photographs of vertical plumes, formed in a deep chamber containing a suspension of the alga, *Chlamydomonas nivalis*, can be seen in Kessler (1986) and Pedley & Kessler (1992), for example. Gyrotactic instability of a uniform suspension of bottom-heavy swimming cells was analysed by Pedley, Hill & Kessler (1988, henceforth referred to as PHK). They assumed that cells are identical prolate spheroids, each swimming at the same prescribed speed V_o relative to the fluid in a direction parallel to its axis of symmetry, represented by the unit vector $\boldsymbol{e}$ that is determined by the gyrotactic torque balance. Randomness of cell swimming behaviour and intrinsic variability between cells was represented by an isotropic cell diffusivity D. The bulk suspension was treated as dilute (no cell-cell interactions) with a Newtonian stress tensor. PHK showed that disturbances with sufficiently long horizontal wavelength (wavenumber $\kappa < \kappa_c$) would always grow, and that the growth rate would be maximum at a particular finite value of $\kappa\,(\kappa_m)$. Quantitatively, the predicted wavelength corresponding to κ_m was somewhat larger than the experimentally observed spacing of plumes, but not outrageously so, given the uncertainty in the estimation of certain parameters.

The model of PHK was *ad hoc*, in that it assumed a deterministic cell swimming direction $\boldsymbol{e}$ concurrently with cell diffusion to represent random cell swimming. Pedley & Kessler (1990, henceforth PK) improved the model by postulating a probability density function (p.d.f.) of cell swimming direction, $f(\boldsymbol{e})$, in terms of which the mean cell swimming direction and the cell diffusivity tensor (no longer isotropic) could be computed. This function was assumed to satisfy a quasi-steady Fokker–Planck equation (a partial differential equation in $\boldsymbol{e}$-space) in which

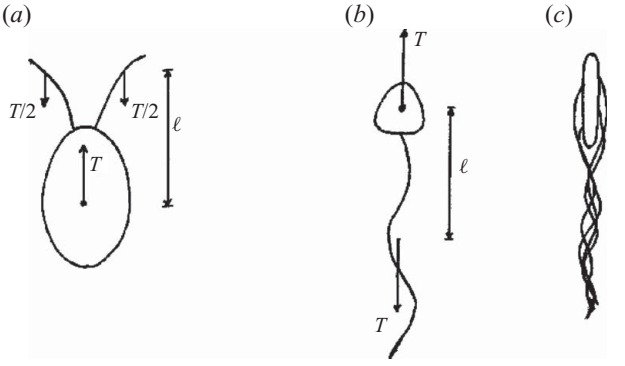

FIGURE 1. Examples of swimming micro-organisms, in which the swimming apparatus exerts a thrust T backwards on the fluid, while the body or head exerts an equal and opposite drag force, in the forwards direction, $\boldsymbol{e}$. The distance between the effective points of application of these forces is ℓ. The force dipole system is equivalent to a stresslet S of magnitude $T\ell$. (a) A biflagellate algal cell, for which $S>0$ (a 'puller'); (b) a spermatozoon and (c) a bacterium, for both of which $S<0$ ('pushers').

random fluctuations in $\boldsymbol{e}$, represented by an isotropic rotational diffusivity, were balanced by the tendency for the gyrotactic torque balance to push $\boldsymbol{e}$ back to its deterministic direction. In addition, PK modified the bulk fluid model by incorporating terms in the stress tensor $\boldsymbol{\Sigma}$ additional to the Newtonian viscous stress. Some of these were the 'Batchelor stresses', present in any particulate suspension, but these proved to have a negligibly small effect on the predicted most unstable wavenumber and growth rate. However, one additional term was not negligible. This term arises because the swimming motion of each cell has an effect on the fluid that, in the far field, is equivalent to a force-dipole or 'stresslet' (it is assumed that the cell Reynolds number is very small, so locomotion is dominated by viscosity).

Figure 1 shows three examples of swimming micro-organisms, in which a cell's swimming apparatus exerts a thrust T backwards on the fluid, while its body or head exerts an equal and opposite drag force in the forwards direction. If the distance between the effective points of application of these forces is ℓ, then the magnitude of the equivalent stresslet is $T\ell$. For a biflagellate algal cell, such as *C. nivalis*, depicted in figure 1(a), the stresslet strength, $S=T\ell$, is positive. Such cells can be thought of as 'pullers', pulling themselves along by their breast-stroke-like flagellar action. The effect on the fluid is to pull it in along the axis of symmetry and push it out sideways in the perpendicular plane. Figure 1(b) represents a spermatozoon, pushed from behind by a waving flagellum, while figure 1(c) represents a bacterial cell, pushed from behind by a rotating flagellar bundle. In these two cases, $S=-T\ell$ and is negative; the cells may be termed 'pushers'. Such cells push fluid out along the axis of symmetry, and suck it in from the sides. When there are n identical cells per unit volume, then the sum of the stresslets makes a contribution to the bulk stress tensor of

$$\boldsymbol{\Sigma}^{(p)} = n\ S\big(\langle \boldsymbol{ee}\rangle - \tfrac{1}{3}\boldsymbol{I}\big), \tag{1}$$

where $\boldsymbol{I}$ is the identity tensor and $\langle X \rangle$ represents the average of X over $\boldsymbol{e}$-space (the unit sphere).

$$\langle X \rangle = \int X f(\boldsymbol{e}) \, \mathrm{d}^2 \boldsymbol{e}. \tag{2}$$

(The rotational diffusion of cells leads to an additional contribution to $\boldsymbol{\Sigma}^{(p)}$, as pointed out by Brenner 1972; Hinch & Leal 1972 and PK. However, it has the same tensorial form as (1) and is small in practice, so can be included by adding a small positive quantity to S.)

PK incorporated $\boldsymbol{\Sigma}^{(p)}$ and the Batchelor stresses into their stability analysis, but limited themselves to assessing the effect on the gravitational instability modes arising in the PHK model. For parameter values relevant to *C. nivalis* this effect was quantitatively modest and no qualitatively novel features were noted. However, one category of disturbance modes ('bend-twist modes' in the language of liquid crystals) was ignored altogether, and the particle stress $\boldsymbol{\Sigma}^{(p)}$ can have a significant effect on these (see below). Moreover, bottom-heavy algae are not the only swimming micro-organisms for which bioconvection has been noted and analysed. The bacterium *Bacillus subtilis*, also slightly denser than water, is chemotactic, swimming up oxygen concentration gradients which it may create itself through its consumption of oxygen. In a shallow chamber, open at the top to the atmosphere, the chemotaxis leads to a higher concentration of cells near the free surface, and this leads, as before, to bioconvection, which has been observed by Kessler (1989) and Kessler *et al.* (1994) and analysed (in linear theory) by Hillesdon & Pedley (1996). However, such bacteria can also be constrained to swim in very thin horizontal layers of fluid, for example above an Agar plate, so variations in cell concentration do not lead to gravitational instability. There may be a mean concentration gradient, along which the cells may tend to swim, on average, or there may be no mean gradient and, if there is enough nutrient for all cells to be active, they may choose to swim in any direction. Interesting 'whorl and jet' patterns have been observed in such systems (Mendelson *et al.* 1999; Dombrowski *et al.* 2004). In these circumstances, the particle stresses may play a vital role in the instabilities that arise.

The importance of particle stresses in generating instability in suspensions of self-propelled particles in the absence of gravity has been noted and analysed by Simha & Ramaswamy (2002, henceforth referred to as SR), and more recently by Saintillan & Shelley (2008) and Subramanian & Koch (2009), henceforth referred to as SS and SK, respectively. See also a recent paper by Baskaran & Marchetti (2009). SR based their analysis on the model of 'flocking', i.e. the tendency of animals such as fish and birds to move coherently in large groups, pioneered by Vicsek *et al.* (1995) and developed at length by Toner & Tu (1998) (see also the review by Toner, Tu & Ramaswamy 2005). In the continuum version of this model, the organisms tend to keep moving at the same speed (relative to a fixed frame of reference) and experience interactions that tend to keep them a constant distance apart (a 'particle pressure' that depends on the cell concentration). SR considered apolar nematic cells as well as polar cells like the present directed swimmers, but we consider only the latter. The basic state whose stability is analysed has all the organisms moving (on average) in the same direction, as for the algal suspension analysed by PHK, although in the SR model this basic state is more an initial condition than a solution of the governing equations. The perturbation to the cells' swimming direction is determined by the transverse component of the linear momentum equation of the organisms, rather than by the angular momentum equation (torque balance), but the effect of the fluid

velocity gradient is represented by the same terms and the equations are quite similar. One difference between the SR model and the PHK model is that, in the former, the swimming speed is allowed to vary. This and other aspects of the flocking model, when applied to micro-organisms, are somewhat questionable (see Discussion), but the essential role played by the particle stresses is the same in both. They can lead to novel instabilities, both growing 'bend-twist' waves and growing 'splay-concentration' modes, as recognized by SR.

This paper re-examines the PHK and PK models for linear instability of a dilute uniform suspension in an unbounded fluid with particle stresses included and looks at all potentially relevant parameter ranges, not only those applicable to bottom-heavy algae. The main new feature of this work, relative to PK, is that the p.d.f. of swimming directions $f(\boldsymbol{e})$ is not taken to be quasi-steady, but may depend on space and time as well as $\boldsymbol{e}$, allowing for a lag in response to external changes. However, as will be seen in § 2, this creates a closure problem, and two different approximation schemes are introduced in order to close the system. In both schemes, the cell swimming term in the cell conservation equation is taken to be advection by the average, not the instantaneous, cell swimming velocity. Also, in both schemes, this velocity is assumed not to be quasi-steady. In one scheme (case I) the particle stress tensor is taken to be quasi-steady, while in the other (case II) it is not. However, the latter case leads in general to a set of equations that are unmanageably cumbersome, so this case is treated only for small values of a parameter, λ, for which rotational diffusion is dominant; this is the case relevant to the (slightly) head-heavy bacteria used in experiments.

In developing the theory, consideration has to be given to the representation of translational diffusion. In general, an *ad hoc* diffusivity tensor is assumed (cf. SS); however, in the limit of strong rotational diffusion D_R, the translational diffusivity is known to be proportional to its inverse, and the derivation of this result from the Fokker–Planck equation is considered.

2. Linear theory

In the following equations, $\boldsymbol{u}$ is the bulk fluid velocity, $\boldsymbol{V}$ is the cell swimming velocity relative to the fluid (supposed averaged over a volume element), V_o is the swimming speed of an individual cell, n is the cell number density, $\boldsymbol{e}$ is the cell orientation unit vector, P is the pressure, ρ, ν are the fluid density and kinematic viscosity, D_H, D_V are the horizontal and vertical components of the cell diffusivity tensor in a still fluid and $\widehat{\boldsymbol{k}}$ is a unit vector in the vertically upward direction (downwards for head-heavy cells). Other quantities will be defined where they arise. The coordinates are (x, y, z), with z vertical.

The continuity equation is

$$\nabla \cdot \boldsymbol{u} = 0, \tag{3}$$

while the Navier–Stokes equation under the Boussinesq approximation is

$$\frac{\partial \boldsymbol{u}}{\partial t} + (\boldsymbol{u} \cdot \nabla)\boldsymbol{u} = -\frac{1}{\rho}\nabla P - n\overline{g}\widehat{\boldsymbol{k}} + \nu\nabla^2\boldsymbol{u} + \frac{1}{\rho}\nabla \cdot \boldsymbol{\Sigma}^{(p)}, \tag{4}$$

where $\boldsymbol{\Sigma}^{(p)}$ is given by (1) and

$$\overline{g} = \pm\, \upsilon g \triangle\rho/\rho, \tag{5}$$

where v is cell volume, $\triangle\rho$ is the difference between cell and fluid density, and g is gravity; in (5) the minus sign is taken (so $\overline{g} < 0$) for head-heavy cells.

The equation of conservation of cells is

$$\frac{\partial n}{\partial t} = -\nabla \cdot \left[n(\boldsymbol{u} + \boldsymbol{V} - V_s \widehat{\boldsymbol{k}}) \right] + D_H \nabla_1^2 n + D_V \frac{\partial^2 n}{\partial z^2}, \tag{6}$$

where $\nabla_1^2 \equiv \partial^2/\partial x^2 + \partial^2/\partial y^2$, $\boldsymbol{V} = V_o \langle \boldsymbol{e} \rangle$ and V_s is the cell sedimentation speed, omitted by PK. Here we have simplified PK's full (but still approximate) description of the translational diffusion tensor,

$$\boldsymbol{D} = V_o^2 \tau \left\langle (\boldsymbol{e} - \langle \boldsymbol{e} \rangle)\, (\boldsymbol{e} - \langle \boldsymbol{e} \rangle) \right\rangle, \tag{7}$$

where τ is the correlation time of a cell's random walk, by ignoring the off-diagonal terms (because they do not play a role in the linear instability theory, as shown by PK) and by taking the diagonal terms to be constant, since their variation does not have a qualitative effect on the results. It should be noted that the assumptions concerning translational diffusion are essentially *ad hoc*, because we are combining two or more sources of random behaviour and supposing that they can be represented by a single, diagonal, diffusion tensor. One source of randomness is the natural variability within a population of swimmers – of swimming speed, stresslet strength, shape, etc. – and the other is the effective rotational diffusivity, brought about by beat-by-beat fluctuations in each cell's swimming apparatus (not Brownian rotation, because the cells are too big). For the case of algae such as *C. nivalis* the population effect is likely to be at least as important as the rotational diffusion. However, for bacteria the latter is likely to be dominant, as discussed below. In this case, it will be shown that the orientation distribution is nearly isotropic, and translational diffusion is also almost isotropic, with a diffusivity

$$D = \tfrac{1}{3} V_o^2 \tau = V_o^2 / 6 D_R \tag{8}$$

(see Berg 1983 and Appendix A). Finally, we should note that the swimming mode known as 'run-and-tumble' employed by many bacteria should not be represented by a diffusivity at all, as shown by SK.

The p.d.f. of swimming direction, $f(\boldsymbol{e}, \boldsymbol{x}, t)$, is given by the following Fokker–Planck equation (cf. (A 1) in Appendix A):

$$\frac{\partial f}{\partial t} + \frac{1}{n} \nabla_x \cdot \left\{ n(\boldsymbol{u} + V_o \boldsymbol{e} - V_s \widehat{\boldsymbol{k}}) f - \boldsymbol{D}_T \cdot \nabla_x (nf) \right\} + \nabla_e \cdot \left\{ \beta \left[\widehat{\boldsymbol{k}} - \left(\widehat{\boldsymbol{k}} \cdot \boldsymbol{e} \right) \boldsymbol{e} \right] f + \frac{1}{2} \boldsymbol{\Omega}_\wedge \boldsymbol{e} f + \alpha_0 \boldsymbol{e} \cdot \widehat{\boldsymbol{E}} \cdot (\boldsymbol{I} - \boldsymbol{e}\boldsymbol{e})\, f \right\} = D_R \nabla_e^2 f, \tag{9}$$

where $\boldsymbol{\Omega}$ and $\widehat{\boldsymbol{E}}$ are the vorticity and strain rate in the flow, and ∇_x, ∇_e are the gradient operators in $\boldsymbol{x}$- and $\boldsymbol{e}$-space, respectively. Here $\boldsymbol{D}_T$ is the contribution to translational diffusivity that is not attributable to rotational diffusion, and will be taken (arbitrarily) to be diagonal (cf. (6)). The inverse gyrotactic time scale β is given by

$$\beta = \frac{gh}{\nu \alpha_\perp}, \tag{10}$$

where h is the distance of the centre of mass behind the centre of buoyancy and $\alpha_0, \alpha_\perp$ are numerical constants, equal to 0 and 6 respectively for a spherical cell body, but equal to 0.31 and 6.80 for a prolate spheroid of axis ratio 1.38, as measured for *C. nivalis*. Note that β is also the angular velocity the cell would have if released from

rest in a horizontal orientation. Note also that the above equations are applicable to head-heavy cells as well as bottom-heavy cells as long as, for the former, we take $\widehat{\boldsymbol{k}}$ directed vertically downwards and $\overline{g}$ in (4) and (5) to be negative; β will remain positive.

The only difference between the above equations and those employed by PK lies in the presence of the top line of (9), which represents the fact that f does not respond instantaneously to temporal or spatial changes in the flow. The solution of (9) is needed to calculate the $\boldsymbol{V} = V_o \langle \boldsymbol{e} \rangle$ term in (6) and, more importantly, the $\langle \boldsymbol{ee} \rangle$ term that arises in the $\boldsymbol{\Sigma}^{(p)}$ term in (4), using (1).

The basic state whose stability is to be analysed is one in which the bulk fluid is at rest ($\boldsymbol{u} = 0$) and the cells have a uniform concentration n_0 and swimming direction $\widehat{\boldsymbol{k}}$. A hydrostatic pressure $P_0(z)$ is required to balance the negative buoyancy term in (4). Small perturbations are introduced, of $O(\epsilon)$ say, and we write

$$n = n_0 + \epsilon n', \quad P = P_0(z) + \epsilon \rho P', \quad f(\boldsymbol{e}, \boldsymbol{x}, t) = f^{(0)}(\boldsymbol{e}) + \epsilon f^{(1)}(\boldsymbol{e}, \boldsymbol{x}, t);$$

we also note that $\boldsymbol{u}$, $\boldsymbol{\Omega}$ and $\widehat{\boldsymbol{E}}$ are all $O(\epsilon)$ quantities. For any random variable X we write $\langle X \rangle = \langle X \rangle^{(0)} + \epsilon \langle X \rangle^{(1)}$, where $\langle X \rangle^{(0,1)}$ are related to $f^{(0,1)}$ by (2). The particle stress tensor $\boldsymbol{\Sigma}^{(p)}$ ((1)) varies because both n and $\langle \boldsymbol{ee} \rangle$ vary, so

$$\boldsymbol{\Sigma}^{(p)} = (n_0 + \epsilon n') S(\langle \boldsymbol{ee} \rangle^{(0)} - \tfrac{1}{3}\boldsymbol{I}) + \epsilon n_0 S \langle \boldsymbol{ee} \rangle^{(1)}. \tag{11}$$

In the basic state the only non-zero terms in (9) are those multiplied by β and by D_R; its solution is

$$f^{(0)}(\boldsymbol{e}) = \Lambda \mathrm{e}^{\lambda \widehat{\boldsymbol{k}} \cdot \boldsymbol{e}} = \Lambda \mathrm{e}^{\lambda \cos\theta} \tag{12}$$

where $\lambda = \beta / D_R$, $\Lambda = \lambda / (4\pi \sinh \lambda)$ (so that $\int f^{(0)}(\boldsymbol{e})\, \mathrm{d}^2\boldsymbol{e} = 1$), and we take coordinates so that

$$\boldsymbol{e} = (\sin\theta \cos\phi,\ \sin\theta \sin\phi,\ \cos\theta);$$

see PK for the details. Using (12), PK also obtained $\langle \boldsymbol{e} \rangle^0 = K_1 \widehat{\boldsymbol{k}}$, $K_1 = \coth\lambda - 1/\lambda$ and $\langle \boldsymbol{ee} \rangle^{(0)}_{11} = \langle \boldsymbol{ee} \rangle^{(0)}_{22} = K_1/\lambda$; $\langle \boldsymbol{ee} \rangle^{(0)}_{33} = 1 - 2K_1/\lambda$.

The first-order equation, for $f^{(1)}$, becomes

$$\begin{aligned} \frac{\partial f^{(1)}}{\partial t} &+ \left(V_o \boldsymbol{e} - V_s \widehat{\boldsymbol{k}} \right) \cdot \nabla_x f^{(1)} - \nabla_x \cdot \left(\boldsymbol{D}_T . \nabla_x f^{(1)} \right) \\ &+ \nabla_e \cdot \left\{ \beta \left[\widehat{\boldsymbol{k}} - \left(\widehat{\boldsymbol{k}} \cdot \boldsymbol{e} \right) \boldsymbol{e} \right] f^{(1)} \right\} - D_R \nabla_e^2 f^{(1)} \\ &= - \nabla_e \cdot \left\{ \left[\frac{1}{2} \boldsymbol{\omega}_\wedge \boldsymbol{e} + \alpha_o \boldsymbol{e} \cdot \boldsymbol{E} \cdot (\boldsymbol{I} - \boldsymbol{ee}) \right] f^{(0)} \right\}, \end{aligned} \tag{13}$$

where $(\boldsymbol{\Omega}, \widehat{\boldsymbol{E}}) = \epsilon(\boldsymbol{\omega}, \boldsymbol{E})$; $\boldsymbol{\omega}$ and $\boldsymbol{E}$ are still dimensional quantities. When this is integrated over $\boldsymbol{e}$-space, the result is the first-order perturbation to the cell conservation equation (6). At this point, we make the arbitrary assumption that the advective term in (13) due to individual cell swimming can be replaced by that due to average cell swimming, and we will neglect translational diffusion in this equation, so the top line becomes

$$\frac{\partial f^{(1)}}{\partial t} + \left(V_o \langle \boldsymbol{e} \rangle^{(o)} - V_s \widehat{\boldsymbol{k}} \right) \cdot \nabla_x f^{(1)}. \tag{14}$$

The main results of this paper, which are obtained for long wavelength, will not be qualitatively affected by these approximations.

The linearized, $O(\epsilon)$, governing equations have constant coefficients and can therefore be analysed in terms of individual Fourier modes; thus, every perturbation variable is taken to be proportional to

$$\exp(\sigma t + \mathrm{i}\boldsymbol{\kappa}\cdot\boldsymbol{x}), \qquad \boldsymbol{\kappa} = (k, l, m).$$

If we multiply (13) by $\boldsymbol{e}$ and integrate over $\boldsymbol{e}$-space, we obtain an equation for $\langle\boldsymbol{e}\rangle^{(1)}$ involving $\langle\boldsymbol{ee}\rangle^{(1)}$ and known quantities (see Appendix A):

$$(\sigma_1 + 2D_R)\langle\boldsymbol{e}\rangle^{(1)} + \beta\widehat{\boldsymbol{k}}\cdot\langle\boldsymbol{ee}\rangle^{(1)} = \tfrac{1}{2}\boldsymbol{\omega}_\wedge\langle\boldsymbol{e}\rangle^{(0)} + \alpha_0\left\{\langle\boldsymbol{e}\rangle^{(0)}\cdot\boldsymbol{E} - \langle\boldsymbol{e}\cdot\boldsymbol{E}\cdot\boldsymbol{ee}\rangle^{(0)}\right\} \equiv \boldsymbol{R}_1, \quad (15)$$

where

$$\sigma_1 = \sigma + \mathrm{i}(K_1 V_0 - V_S)m. \quad (16)$$

Similarly, if we multiply (13) by $\boldsymbol{ee}$ and integrate, we obtain the following equation for $\langle\boldsymbol{ee}\rangle^{(1)}$ in terms of known quantities $\langle\boldsymbol{e}\rangle^{(1)}$ and the unknown quantity $\langle\boldsymbol{eee}\rangle^{(1)}$:

$$\begin{aligned}(\sigma_1 + 6D_R)\langle\boldsymbol{ee}\rangle^{(1)} - \beta\big(\langle\boldsymbol{e}\rangle^{(1)}\widehat{\boldsymbol{k}} + \widehat{\boldsymbol{k}}\langle\boldsymbol{e}\rangle^{(1)}\big) + 2\beta\langle\big(\widehat{\boldsymbol{k}}\cdot\boldsymbol{e}\big)\boldsymbol{ee}\rangle^{(1)} \\ = \tfrac{1}{2}\langle\boldsymbol{e}\,\boldsymbol{\omega}_\wedge\boldsymbol{e} + \boldsymbol{\omega}_\wedge\boldsymbol{ee}\rangle^{(0)} + \alpha_0\langle\boldsymbol{e}\,(\boldsymbol{e}\cdot\boldsymbol{E}) + (\boldsymbol{e}\cdot\boldsymbol{E})\,\boldsymbol{e} - 2\,(\boldsymbol{e}\cdot\boldsymbol{E}\cdot\boldsymbol{e})\,\boldsymbol{ee}\rangle^{(0)} \equiv \boldsymbol{R}_2. \quad (17)\end{aligned}$$

Since an explicit solution of (13) is unavailable in general, the averaging process must be truncated or approximated at some stage. PK did integrate (13) explicitly for the quasi-steady case in which $\sigma_1 = 0$, and hence could calculate $\langle\boldsymbol{e}\rangle^{(1)}$ and $\langle\boldsymbol{ee}\rangle^{(1)}$ for use in (6) and (11). The simplest way to extend that solution would be to use PK's result to calculate $\langle\boldsymbol{ee}\rangle^{(1)}$ in (11) and (15), so the particle stress will remain quasi-steady, and then use (15) to calculate $\langle\boldsymbol{e}\rangle^{(1)}$, so only $\langle\boldsymbol{e}\rangle^{(1)}$ is changed and is not quasi-steady. We will refer to this approximation as case I, and the fullest analysis of the results will be given for this case.

The next level of approximation would be to use PK's solution for $f^{(1)}$ to calculate $\langle(\widehat{\boldsymbol{k}}\cdot\boldsymbol{e})\boldsymbol{ee}\rangle^{(1)}$ in (17), and then combine (15) and (17) to obtain equations for $\langle\boldsymbol{e}\rangle^{(1)}$ and $\langle\boldsymbol{ee}\rangle^{(1)}$ only. However, the manipulations in this case rapidly become extremely cumbersome in general, so here we restrict attention to small values of λ, as is appropriate for bacteria and spermatozoa (see table 2). Since $\beta = \lambda D_R$, this also means small β. We shall not make any further truncation assumption, apart from those implicit in the small-λ approximation, but in this case rotational diffusion is clearly dominant, and we neglect $\boldsymbol{D}_T$. In the case $\beta = 0$, it is simple to write down the exact solution of (14) and (16):

$$\langle\boldsymbol{e}\rangle^{(1)} = \frac{\boldsymbol{R}_1}{\sigma_1 + 2D_R}, \quad \langle\boldsymbol{ee}\rangle^{(1)} = \frac{\boldsymbol{R}_2}{\sigma_1 + 6D_R}; \quad (18)$$

for $\overline{g} = 0$ also, this (effectively) was the case considered by SR, SS and SK. However, we might recall that if $\beta = 0$ there is no reason for the cells to swim in the same direction initially, so SR's basic state is highly artificial at low volume fraction (though not for high volume fractions of rodlike cells, for example, as envisaged by SR), and it comes as no surprise to find that it is unconditionally unstable. When β and λ are zero, the basic state is one of isotropic random swimming, and the development of patterns from that initial state, with $\beta = \overline{g} = 0$, has recently been investigated in detail by SS for a system in which the translational diffusion in (9) is independent of rotational diffusion. We will denote our small-λ expansion as case II.

If we write

$$\boldsymbol{u} = \epsilon(u, v, w), \quad \langle\boldsymbol{e}\rangle^{(1)} = e_i' \text{ and } \langle\boldsymbol{ee}\rangle^{(1)} = Y_{ij},$$

the perturbations to (3), (4) and (6) become as follows:

$$ku + \ell\upsilon + mw = 0, \tag{19}$$

$$(\sigma + \nu\kappa^2)u = -\mathrm{i}kP' - \frac{\mathrm{i}SK_3}{3\rho}kn' + \frac{\mathrm{i}n_0S}{\rho}(kY_{11} + lY_{12} + mY_{13}), \tag{20a}$$

$$(\sigma + \nu\kappa^2)v = -\mathrm{i}\ell P' - \frac{\mathrm{i}SK_3}{3\rho}\ell n' + \frac{\mathrm{i}n_0S}{\rho}(kY_{21} + \ell Y_{22} + mY_{23}), \tag{20b}$$

$$(\sigma + \nu\kappa^2)w = -\mathrm{i}mP' - \bar{g}n' + \frac{2\mathrm{i}SK_3}{3\rho}mn' + \frac{\mathrm{i}n_0S}{\rho}(kY_{31} + \ell Y_{32} + mY_{33}), \tag{20c}$$

$$[\sigma + D_H(\kappa^2 - m^2) + D_V m^2 + \mathrm{i}(K_1V_0 - V_s)m]n' = -\mathrm{i}n_0V_0(ke_1' + \ell e_2' + me_3'). \tag{21}$$

These are supplemented by the equations that give e_i' and Y_{ij} in terms of the vorticity and strain rate, ω and $\boldsymbol{E}$, appropriate to the case studied, I or II. The equations will then be seen to be 5 equations for 5 unknowns (u, υ, w, P', n'), and can be combined to form polynomial equations for the growth rate σ. One set of modes ('twist' modes) can be examined by taking the vertical component of the curl of (4), k (20b) $-$ ℓ (20a), and another set ('splay' modes) by taking its divergence, k (20a) + ℓ (20b) + m (20c). The resulting equations depend on which of the above truncation approximations is used.

Case I

Here $\boldsymbol{Y}$ is given by PK's formulae for $\langle \boldsymbol{ee} \rangle^{(1)}$. The twist operation yields a single homogeneous equation for the z-component of vorticity, $\mathrm{i}(k\upsilon - \ell u)$. We non-dimensionalize with respect to micro-organism swimming time- and length scales, writing

$$\sigma = \frac{V_0^2}{D_H}\sigma', \quad \kappa = \frac{V_0}{D_H}\kappa', \quad \mu = \frac{m}{\kappa}, \tag{22}$$

and obtain

$$\sigma' = -\widehat{\nu}\kappa'^2 - \frac{\widehat{S}\kappa'^2}{2}\left\{J_2\mu^2 - \alpha_0\left[\frac{1}{2}J_6(1-\mu^2) + J_5\mu^2\right]\right\}, \tag{23}$$

where

$$\widehat{\nu} = \frac{\nu}{D_H}, \quad \widehat{S} = \frac{n_0S}{\rho V_0^2}. \tag{24}$$

Note that μ is the cosine of the angle between the wavenumber vector and the vertical. Also, the constants J_i, like K_i, are functions of λ defined in PK.

In this case, the splay modes lead to the following cubic equation for σ':

$$(\widetilde{\sigma} + 2\widehat{D}_R)\left[\widetilde{\sigma} + \kappa'^2(1 - \mu^2 + \widehat{D}_V\mu^2)\right]\left[\widetilde{\sigma} - \mathrm{i}\widehat{V}\kappa'\mu + \widehat{\nu}\kappa'^2 - \widehat{S}\kappa'^2B_1(\mu)\right] - \kappa'^2(1-\mu^2)(\widehat{g} - \mathrm{i}K_3\widehat{S}\kappa'\mu)B_2(\mu) = 0, \tag{25}$$

where

$$B_1(\mu) = \tfrac{1}{2}J_2(1 - 2\mu^2) + \tfrac{1}{2}\alpha_0\left\{J_5(1-2\mu^2)^2 + \tfrac{1}{2}(J_6 + 9K_5)\mu^2(1-\mu^2)\right\} \tag{26a}$$

and

$$B_2(\mu) = +\frac{1}{2}(K_1 - \widehat{\beta} J_2) - \frac{\alpha_0}{2}\left\{K_1(1-2\mu^2) - \frac{2K_3}{\lambda}(1-5\mu^2) + \widehat{\beta} J_5(1-2\mu^2) + \widehat{\beta}\alpha_0 K_5 3\mu^2\right\} \quad (26b)$$

and the new dimensionless parameters are

$$\widehat{g} = \frac{n_0 \overline{g} D_H}{V_0^3}, \quad \widehat{\beta} = \frac{\beta D_H}{V_0^2}, \quad \widehat{D}_V = \frac{D_V}{D_H}, \quad \widehat{D}_R = \frac{D_H}{V_0^2} D_R, \quad \widehat{V} = K_1 - \frac{V_S}{V_0}, \quad (27)$$

and

$$\tilde{\sigma} = \sigma' + \mathrm{i}\widehat{V}\kappa'\mu. \quad (28)$$

We may note that the last, B_2, term in (25) arises from the cell conservation equation; when that term is zero or negligible, then fluctuations in cell concentration are not important to any instability. We should also note an important difference between the above equations (and those used by PK) and the corresponding equations used by SR and SS. The difference stems from the perturbation of the particle stress due to the perturbation of $\langle \boldsymbol{ee} \rangle$. We (and PK) calculate $\langle \boldsymbol{ee} \rangle^{(1)}$ on the basis of the perturbed p.d.f. for $\boldsymbol{e}$, given by (an approximation to) the Fokker–Planck equation (9) (or (13)). On the other hand, SR and SS did not perform the averaging, but effectively replaced $\langle \boldsymbol{ee} \rangle$ by $\boldsymbol{ee}$ and set $\boldsymbol{e} = \widehat{\boldsymbol{k}} + \epsilon \boldsymbol{e}'$, where $\boldsymbol{e}'$ is given by the deterministic equation

$$\frac{\partial \boldsymbol{e}'}{\partial t} + V_0 \frac{\partial \boldsymbol{e}'}{\partial z} = -\beta \boldsymbol{e}' + \frac{1}{2}\,\boldsymbol{\omega} \wedge \widehat{\boldsymbol{k}}$$

(where we have neglected D_T and have set $\alpha_0 = 0$ for convenience). Thus,

$$(\sigma + \mathrm{i}V_0 m + \beta)(\boldsymbol{e}_1', \boldsymbol{e}_2') = \tfrac{1}{2}\,(\omega_2, -\omega_1),$$

which is essentially the same as obtained from (15) and (16), but the non-zero terms of the perturbation to $\boldsymbol{Y} = \boldsymbol{ee}$, i.e. $\boldsymbol{ke}' + \boldsymbol{e}'\boldsymbol{k}$, are $Y_{13} = Y_{31} = e_1'$ and $Y_{23} = Y_{32} = e_2'$. Hence, the B_1, B_2 terms on the right-hand side of (25) are divided by $(\tilde{\sigma} + \widehat{\beta})$, with $J_2 = 1$. These terms are much easier to calculate using this model, and therefore do allow for unsteadiness in the particle stress tensor. The order of the dispersion relation, (23) or (25), is increased by one, the terms $(\tilde{\sigma} - \mathrm{i}\widehat{V}\kappa'\mu + \widehat{\nu}\kappa'^2)$ and $\widehat{g}$ being multiplied by $(\tilde{\sigma} + \widehat{\beta})$.

Case II ($\lambda \ll 1$)

Here we revert to the full Fokker–Planck equation (13), modified by (14), for the first-order probability distribution function $f^{(1)}$; the intention is to solve for $f^{(1)}$, and the quantities that depend upon it, to $O(\lambda)$. Writing $f^{(1)} = f_0^{(1)} + \lambda f_1^{(1)} + \cdots$, and noting from (12) that

$$f^{(0)} = \frac{1}{4\pi}(1 + \lambda \cos\theta + O(\lambda^2)),$$

we obtain

$$-D_R \nabla_e^2 f_0^{(1)} + \sigma_1 f_0^{(1)} = \frac{3\alpha_0}{4\pi D_R} F_1(\theta, \phi), \quad (29a)$$

$$-D_R \nabla_e^2 f_1^{(1)} + \sigma_1 f_1^{(1)} = \frac{D_R}{\sin\theta}\frac{\partial}{\partial\theta}\left(\sin^2\theta f_0^{(1)}\right) + \frac{\sin\theta}{8\pi}(\omega_2 \cos\phi - \omega_1 \sin\phi) + \frac{\alpha_0 \sin\theta}{4\pi} F_2(\theta, \phi) + \frac{3\alpha_0 \cos\theta}{4\pi} F_1(\theta, \phi), \quad (29b)$$

where θ, ϕ are spherical polar angles in $\boldsymbol{e}$-space,

$$\left.\begin{aligned} \nabla_e^2 f &= \frac{1}{\sin\theta}\frac{\partial}{\partial\theta}\left(\sin\theta\frac{\partial f}{\partial\theta}\right) + \frac{1}{\sin^2\theta}\frac{\partial^2 f}{\partial\phi^2}, \\ F_1(\theta,\phi) &= \frac{1}{2}\,E_{33}(3\cos^2\theta - 1) + \left[\frac{1}{2}\,(E_{11}-E_{22})\cos 2\phi \right. \\ &\quad \left. + E_{12}\sin 2\phi\,\right]\sin^2\theta + (E_{13}\cos\phi + E_{23}\sin\phi)\sin 2\theta, \\ F_2(\theta,\phi) &= -\frac{3}{4}E_{33}\sin 2\theta + \left[\frac{1}{4}\,(E_{11}-E_{22})\cos 2\phi \right. \\ &\quad \left. + \frac{1}{2}\,E_{12}\sin 2\phi\,\right]\sin 2\theta + (E_{13}\cos\phi + E_{23}\sin\phi)\cos 2\theta; \end{aligned}\right\} \tag{30}$$

see PK for further details. The solutions of (29*a*) and 29*b*) are

$$f_0^{(1)} = \frac{3\alpha_0}{4\pi(\sigma_1 + 6D_R)}F_1(\theta,\phi), \tag{31a}$$

$$\begin{aligned} f_1^{(1)} = {} & \frac{\sin\theta}{8\pi(\sigma_1+2D_R)}(\omega_2\cos\phi - \omega_1\sin\phi) - \frac{\alpha_0}{4\pi(\sigma_1+6D_R)(\sigma_1+12D_R)} \\ & \times\left\{3E_{33}\cos\theta\left[-2(\sigma_1+9D_R)\cos^2\theta + \frac{(\sigma_1^2+16\sigma_1 D_R+24D_R^2)}{\sigma_1+2D_R}\right]\right. \\ & -2(\sigma_1+9D_R)\,[(E_{11}-E_{22})\cos 2\phi + 2E_{12}\sin 2\phi]\cos\theta\sin^2\theta \\ & \left.+(E_{13}\cos\phi + E_{23}\sin\phi)\sin\theta\left[-8(\sigma_1+9D_R)\cos^2\theta + \frac{\sigma_1(\sigma_1+8D_R)}{\sigma_1+2D_R}\right]\right\}. \end{aligned} \tag{31b}$$

These functions are then used to evaluate $\boldsymbol{e}' = \langle\boldsymbol{e}\rangle^1$ and $\boldsymbol{Y} = \langle\boldsymbol{ee}\rangle^1$ to $O(\lambda)$, as needed in (20) and (21):

$$\boldsymbol{e}' = \frac{\lambda}{\sigma_1+2D_R}\left[\frac{1}{6}\begin{pmatrix}\omega_2\\-\omega_1\\0\end{pmatrix} + \frac{\alpha_0(\sigma_1+4D_R)}{5(\sigma_1+6D_R)}\begin{pmatrix}E_{13}\\E_{23}\\E_{33}\end{pmatrix}\right], \tag{32a}$$

$$\boldsymbol{Y} = \frac{2\alpha_0}{5(\sigma_1+6D_R)}\,\boldsymbol{E} + O(\lambda^2). \tag{32b}$$

It can be seen that all the factors involving the inverse of $(\sigma_1 + CD_R)$ (where $C = 2$ or 6) will complicate the equation for the growth rate, but it is these factors that represent the non-quasi-steadiness of the orientation distribution.

Using the expressions (32*a*) and (29*b*) in the governing equations (19)–(21), and non-dimensionalizing as for case I, we obtain the analogues of (23) and (25) for the twist and splay modes, respectively. For the twist modes, we have

$$\sigma' + \hat{\nu}\kappa'^2 + \frac{\alpha_0\hat{S}\kappa'^2}{5(\tilde{\sigma}+6\hat{D}_R)} = 0, \tag{33}$$

differing from the $O(\lambda)$ expansion of (23) only in the numerical factor and $(\tilde{\sigma}_1+6D_R)^{-1}$ that multiply the last term (see Appendix B for the small-λ expansions of the constants J_i).

Thus, σ' satisfies a quadratic equation

$$(\tilde{\sigma}+6\hat{D}_R)(\tilde{\sigma} - \mathrm{i}\hat{V}\kappa'\mu + \hat{\nu}\kappa'^2) + \frac{\alpha_0\hat{S}}{5}\kappa'^2 = 0, \tag{34}$$

where we recall that $\tilde{\sigma} = \sigma' + \mathrm{i}\hat{V}\kappa'\mu$.

Parameter	(units)	*C. nivalis*	*B. subtilis* (chemotactic)	*B. subtilis* (sedimenting)	Spermatozoa (sedimenting)
ρ	(g cm^{-3})	1	1	1	1
g	(cms^{-2})	980	980	980	980
ν	(cm^{2}s^{-1})	0.011	0.011	0.011	0.011
$\triangle\rho/\rho$	(1)	0.05	0.10	0.10	0.30
υ	(cm^3)	2.1×10^{-9}	1.5×10^{-12}	1.5×10^{-12}	1.4×10^{-11}
$\overline{g} = \upsilon g \triangle\rho/\rho$	(cm^{4}s^{-2})	10^{-7}	0	-1.5×10^{-10}	-4×10^{-9}
n_0	(number cm^{-3})	10^6	10^9	10^9	?
$\alpha_\perp$	(1)	6.8	n.a.	n.a.	n.a.
h	(cm)	10^{-5}	n.a.	n.a.	n.a.
$\beta = gh/\nu\alpha_\perp$	(s^{-1})	0.16	> 0	1.4×10^{-3}	0.02
V_0	(cms^{-1})	6×10^{-3}	2×10^{-3}	2×10^{-3}	3×10^{-3}
V_S	(cms^{-1})	6×10^{-4}	2×10^{-6}	2×10^{-6}	4.4×10^{-5}
S	(g cm^{2}s^{-2})	10^{-10}	-2.7×10^{-11}	-2.7×10^{-11}	-2.2×10^{-10}
D_H	(cm^{2}s^{-1})	1.3×10^{-5}	1.33×10^{-6}*	1.33×10^{-6}*	3.0×10^{-6}*
D_V	(cm^{2}s^{-1})	8.2×10^{-6}	$\leqslant D_H$	$\leqslant D_H$	$\leqslant D_H$
D_R	(s^{-1})	0.073	0.5	0.5	0.5
α_0	(1)	0.31	0.78	0.78	0.9?

TABLE 1. Parameter values. *For bacteria and spermatozoa D_H is calculated from (7), with an arbitrarily assumed correlation time τ of 1 s. n.a., not applicable; ?, doubtful/unknown.

The splay modes are more complicated. We note that, to $O(\lambda)$, $\langle \boldsymbol{e} \rangle^{(0)} = 0$, so (32$a$) gives the leading term for $\langle \boldsymbol{e} \rangle$, while $\langle \boldsymbol{ee} \rangle^{(0)}$ and the diffusivity tensor are isotropic, so $\widehat{D}_V = 1$. The equation for the growth rate, corresponding to (25), becomes

$$(\widetilde{\sigma} + 2\widehat{D}_R)(\widetilde{\sigma} + \kappa'^2)\left[(\widetilde{\sigma} - \mathrm{i}\widehat{V}\kappa'\mu + \widehat{\nu}\kappa'^2 + \frac{\alpha_0 \widehat{S}\kappa'^2}{5(\widetilde{\sigma} + 6\widehat{D}_R)}\right] = \lambda\widehat{g}\kappa'^2(1-\mu^2)\left[\frac{1}{6} - \frac{\alpha_0(\widetilde{\sigma} + 4\widehat{D}_R)}{10(\widetilde{\sigma} + 6\widehat{D}_R)}\right], \quad (35)$$

which is a fourth-order algebraic equation, to be contrasted with the third-order equation in case I.

3. Parameter values

Table 1 lists parameter values pertaining to the two types of micro-organisms discussed above: biflagellate algal cells, *C. nivalis*, in the concentrations used in bioconvection experiments, with three additional columns for sedimenting non-chemotactic bacteria and spermatozoa, as representatives of head-heavy cells, and for chemotactic bacteria ($\beta > 0$) in the absence of gravity ($\overline{g} = 0$). The concentrated bacterial suspensions that generate whorls and jets (Mendelson *et al.* 1999) would have $\beta = 0$ and $\overline{g} = 0$; in these experiments, the number density n_0 of around 10^{11} cm^{-3} was 100 times larger than that in the 'bacterial bioconvection' experiments of Kessler (1989). Most of the parameters can be obtained from PHK, Pedley & Kessler (1990, 1992), Kessler (1989), Hillesdon, Pedley & Kessler (1995) and Bretherton & Rothschild (1961). In the case of chemotactic bacteria, to model the tendency to swim in a given direction as an effective restoring torque is entirely *ad hoc* and all that can be said about the corresponding value of β is that it should be positive.

Parameter	*C. nivalis*	*B. subtilis* (chemotactic)	*B. subtilis* (sedimenting)	Spermatozoa (sedimenting)
$\widehat{\nu} = \nu/D_H$	850	8500	8500	3700
$\widehat{D}_V = D_V/D_H$	0.63	1 ?	1 ?	1 ?
$\widehat{D}_R = D_R D_H/V_0^2$	0.026	0.17	0.17	0.17
$\widehat{V} = K_1 - \dfrac{V_S}{V_0}$	0.47	?	1.9×10^{-3}	2.8×10^{-2}
$\widehat{S} = \dfrac{n_0 S}{\rho V_0^2}$	2.8	−6700	−6700	$-2.4 \times 10^{-5} n_0$
$\widehat{g} = \dfrac{n_0 \overline{g} D_H}{V_0^3}$	38	0	−25	$-4.4 \times 10^{-5} n_0$
$\widehat{\beta} = \beta D_H/V_0^2$	0.058	$? > 0$	4.7×10^{-4}	6.7×10^{-4}
$\lambda = \beta/D_R$	2.2	?	2.8×10^{-3}	4.0×10^{-2}

TABLE 2. Dimensionless derived parameters.

Quantity	$\lambda = 2.2$	$\lambda \ll 1$
Λ	25.46	$\dfrac{1}{4\pi}(1 - \lambda^2/6)$
K_1	0.57	$\dfrac{\lambda}{3}(1 - \lambda^2/15)$
K_3	0.22	$\dfrac{\lambda^2}{15}\left(1 - \dfrac{2\lambda^2}{21}\right)$
K_5	−0.11	$-\dfrac{2\lambda}{45}\left(1 + \dfrac{2\lambda^2}{21}\right)$
J_2	0.16	$\dfrac{\lambda^3}{36}$
J_5	−0.13	$-\dfrac{\lambda}{15}\left(1 + \dfrac{\lambda^2}{21}\right)$
J_6	−0.20	$-\dfrac{2\lambda}{15}\left(1 - \dfrac{2\lambda^2}{21}\right)$

TABLE 3. Functions of λ, for $\lambda = 2.2$ (*C. nivalis*) and for small λ (mostly from PK).

However, for non-chemotactic, head-heavy bacteria or spermatozoa in a gravitational field, the magnitude of β is calculated from resistive force theory as the initial angular velocity when these organisms are released from rest in a horizontal orientation. We recall that, in these cases, the only quantity that changes sign is $\overline{g}$. Table 2 lists the dimensionless parameters that appear in (22)–(35) and are the relevant ones for this stability analysis; the large negative values of $\widehat{S}$ for bacteria are a consequence of the assumed cell number density n_0, from the experiments reported by Kessler (1989) and Kessler *et al.* (1994). It will be noted that sedimentation affects only the advective, $\widehat{V}$, terms in (23), (25), (34) and (35). We also note that we have no information on the anisotropy of the cell diffusion tensor for bacteria and, for simplicity, we shall take $\widehat{D}_V = 1$ in most cases, since this is its value in the small λ limit. However, the rotational diffusivity for small λ is related to the translational diffusivity as already discussed (see (8)).

The values of the various functions of λ that arise in equations between (16) and (28), i.e. J_i, K_i, are given in table 3, where relevant. In many cases, λ is thought to

be very small, so the first terms in the small-λ expansion are given in table 3. The functions $B_1(\mu)$, $B_2(\mu)$ from (26*a*) and (26*b*) are given in Appendix B: it can be seen that, for small λ, B_1 is negative unless $\alpha_0 = 0$ (spherical cells) and $\mu^2 > 1/2$, while B_2 is positive unless both α_0 and μ^2 are sufficiently close to 1, i.e. elongated cells and wavenumber with a sufficiently large vertical component.

4. Results

In this section detailed results are given for cases I and II. In both cases, we will present some analytical results in relevant asymptotic limits, such as long wavelength ($\kappa' \to 0$) and large Schmidt number ($\widehat{\nu} \to \infty$; see table 2), before supplementing them with numerical results from the full eigenvalue equation (e.g. (23) or (25)) for particular parameter values.

4.1. *Case I (unsteady mean orientation, quasi-steady particle stress)*

Consider first the 'twist' mode, ignored by PHK and PK, for which the growth rate is given by (23). The constants J_5 and J_6 are negative (see table 3), so it can be seen that σ' is negative, indicating stability, for $\widehat{S} > 0$, i.e. for pullers such as *Chlamydomonas* (thus the neglect of this mode by PHK and PK did not cause any instability to be missed). However, σ' can be positive if $\widehat{S} < 0$ (pushers) as long as $|\widehat{S}|$ is large enough, i.e.

$$\frac{\widehat{\nu}}{|\widehat{S}|} \quad < \quad \underset{0 \leqslant \mu^2 \leqslant 1}{Max} \left\{ -\frac{\alpha_0}{4} J_6 + \mu^2 \left(\frac{1}{2} J_2 - \frac{\alpha_0}{2} J_5 + \frac{\alpha_0}{4} J_6 \right) \right\}. \tag{36}$$

This mode of instability was postulated by SR. The right-hand side of (36) is equal to $(1/2)J_2\mu^2$ for $\alpha_0 = 0$ (spherical cells), indicating that the most unstable mode has vertical wavenumber ($\mu = 1$), but the maximum may occur for $\mu^2 < 1$, even $\mu^2 = 0$, in some cases with $\alpha_0 \neq 0$. In particular, the parameters for sedimenting *B. subtilis* (or spermatozoa) given in table 2 show that the right-hand side of (36) is approximately 1.5×10^{-4} (or 1.2×10^{-3}), whereas $\widehat{\nu}/|\widehat{S}|$ is greater than 1, so a *B. subtilis* suspension, at the assumed value of n_0, (or a sperm suspension at any realistic n_0) would not be unstable to this mode. This will be the case even for concentrated bacterial suspensions, with n_0 100 times larger.

Now consider the 'splay' modes given by (25). Given the large size of $\widehat{\nu}$ in realistic examples (table 2), it is sensible first to consider the limit of (25) in which $\widehat{\nu}\kappa'^2$ is much larger than the other terms in the square bracket containing it; this corresponds to the Stokes limit in which inertia is negligible in the bulk flow as well as for individual swimmers. Then (25) (with $\widehat{D}_V = 1$ for convenience) reduces to

$$\widetilde{\sigma}^2 + \widetilde{\sigma}(2\widehat{D}_R + \kappa'^2) + 2\widehat{D}_R\kappa'^2 - (\widehat{g}/\widehat{\nu} - \mathrm{i}K_3 \frac{\widehat{S}}{\widehat{\nu}}\kappa'\mu)(1-\mu^2)B_2(\mu) = 0. \tag{37}$$

We see immediately that $R_e(\widetilde{\sigma}) > 0$ if

$$\frac{\widehat{g}}{\widehat{\nu}}(1-\mu^2)B_2(\mu) > 2\widehat{D}_R\kappa'^2, \tag{38}$$

and since $B_2(\mu)$ is positive for all μ, in all the cases listed in table 2, and in general for small λ, there is (gyrotactic) instability for positive $\widehat{g}$ and $\mu \neq 1$ at small enough wavenumber κ'. Moreover, $R_e(\widetilde{\sigma})$ is necessarily negative (stability) if $\widehat{g} < 0$ and κ' is small enough, whatever the sign of $\widehat{S}$. However, if $\widehat{g} = 0$, then the leading terms in the

small-κ' expansion for $\widetilde{\sigma}$ from (37) take the form

$$\widetilde{\sigma} = -\mathrm{i}\sigma_1\kappa' - \left(1 - \frac{\sigma_1^2}{2\widehat{D}_R}\right)\kappa'^2, \tag{39}$$

where $\sigma_1 = K_3(\widehat{S}/2\widehat{\nu}\widehat{D}_R)\mu(1-\mu^2)B_2(\mu)$. Hence, there is a weak instability if $\widehat{S}/\widehat{\nu}$ is large enough whatever its sign. This instability comes from the SK_3 terms in the Navier–Stokes equation (20), i.e. from the perturbation to the particle stress tensor due to fluctuations in volume fraction multiplied by the basic state particle stress. In the absence of rotational diffusivity, this instability will occur for all values of the ratio $\widehat{S}/\widehat{\nu}$, and is the same as that predicted by SR and SS. When D_R is non-zero, there is a critical value of $\widehat{S}/\widehat{\nu}$ given by

$$\frac{\widehat{S}}{\widehat{\nu}} = \frac{(2\widehat{D}_R)^{3/2}}{\mathrm{Max}\,[K_3\mu(1-\mu^2)B_2]}. \tag{40}$$

If we take $\widehat{S}$ of the same (large) order as $\widehat{\nu}$, then in the above discussion $\widehat{\nu}$ is replaced by $\widehat{\nu} - \widehat{S}B_1(\mu)$, these $\widehat{S}$ terms being due to the perturbation in $\langle \boldsymbol{ee} \rangle$, not in n. Hence, if $\widehat{S}B_1(\mu) > \widehat{\nu}$, the stable and unstable modes change round. Since $B_1(\mu) < 0$ in virtually all realistic cases, and always for μ close to 1, it follows that strong pushers can drive instability for such modes even for $\widehat{g} < 0$. Conversely, since $B_1(\mu)$ can be >0 for μ close to zero when α_0 is small and strong, nearly spherical pullers can drive instability even for $\widehat{g} < 0$ (although the existence of head-heavy pullers is questionable; see figure 1), but only if $|\widehat{S}|/\widehat{\nu}$ is large enough to make them happen. For the cases listed in table 2 and Appendix B, $|\widehat{S}|/\widehat{\nu}$ is not larger than $1/|B_1(\mu)|$ (see Discussion).

A little more insight can be gained by performing a small-κ' expansion with all other parameters (including $\widehat{\nu}$ and $\widehat{S}$) taken to be $O(1)$, so inertia is not totally neglected. Now the three roots of (25) are, approximately,

$$\widetilde{\sigma} = -2\widehat{D}_R$$

and

$$\widetilde{\sigma} \approx \frac{\kappa'}{2}\left\{\mathrm{i}\widehat{V}\mu \pm \left[-\widehat{V}^2\mu^2 + \frac{2(1-\mu^2)B_2(\mu)\widehat{g}}{\widehat{D}_R}\right]^{1/2}\right\}. \tag{41}$$

As long as B_2 is positive and μ is taken small enough, this always gives instability if $\widehat{g} > 0$, and this is the gyrotactic instability of PHK; B_2 is positive, for all μ, in all the cases listed in table 2, and in general for small λ unless $\widehat{\beta}$ is very large (Appendix B), which is unrealistic. For $\mu \neq 0$, we see from (41) that the term representing advection (and sedimentation) can stabilize the gyrotactic instability, if $\widehat{g}$ is small enough, at sufficiently small wavenumber for both viscosity and the particle stress to be negligible.

For $\widehat{g} \leqslant 0$, (41) gives neutral stability, so it is necessary to go to the next order in κ'. We write $\widehat{g} = -G$ and take $\widehat{D}_V = 1$, and obtain

$$\widetilde{\sigma} = \kappa\sigma_1 + \kappa^2\sigma_2 \cdots, \tag{42a}$$

where

$$\sigma_1 = \frac{1}{2}\mathrm{i}\left\{\widehat{V}\mu \pm \sqrt{\widehat{V}^2\mu^2 + \frac{2B_2G}{\widehat{D}_R}(1-\mu^2)}\right\} \tag{42b}$$

and

$$(\pm\sqrt{\ })\,\sigma_2 = \frac{1}{2}(\widehat{V}\mu \pm \sqrt{\ })\left\{\frac{B_2 G}{4\widehat{D}_R^2}(1-\mu^2) - \widehat{\nu} - 1 + B_1\widehat{S}\right\} + \widehat{V}\mu - \mu(1-\mu^2)\frac{B_2 K_3 \widehat{S}}{2\widehat{D}_R}; \quad (42c)$$

we recall that there will be instability if $\sigma_2 > 0$. In the limit $\mu = 1$, for which B_1 is negative ((26a) and Appendix B) and G is removed from the equation, the upper sign in (42c) gives instability if (and only if)

$$\widehat{S} < -\frac{\widehat{\nu}}{|B_1|}, \quad (43a)$$

i.e. only pushers give instability, but not unless $-\widehat{S}/\widehat{\nu}$ is sufficiently large; this instability was discussed above. However, for sedimenting *B. subtilis*, $|B_1| \sim 7 \times 10^{-5}$, so again, as for the twist mode, viscosity will suppress the instability in practice (see Discussion). In the limit $\mu = 0$ and $G > 0$, (42c) reduces to

$$\sigma_2 = \frac{1}{2}\left(\frac{B_2 G}{4\widehat{D}_R^2} - \widehat{\nu} - 1 + B_1\widehat{S}\right), \quad (43b)$$

where, in this limit, B_2 is still positive, whereas B_1 may be either positive (e.g. for *C. nivalis*) or negative (e.g. for *B. subtilis*); see table 2 and (26a). It follows, interestingly, both that the gravitational term contributes positively to the instability, even for head-heavy swimmers, and that, when $B_1(0) > 0$, pullers ($\widehat{S} > 0$) would, if head-heavy pullers existed, be more likely to give instability than pushers. From (42c) we can calculate the values of μ for which $\sigma_2 > 0$, for particular parameter values. For example, when $\widehat{g} = -25$, $\widehat{S} = 1$, $\widehat{\nu} = 10$, $\alpha_0 = 0.9$, $\lambda = 1$ (so $\widehat{\beta} = \widehat{D}_R = 1/6$), we find $\sigma_2 > 0$ for μ up to approximately 0.61. It should be recalled that all these instabilities for $\widehat{g} \leqslant 0$ at low wavenumbers are much weaker than the gyrotactic instability for $\widehat{g} > 0$, in that the latter has $R_e(\tilde{\sigma}) = O(\kappa')$ (from (41)) or $O(1)$ (from (37)) while the former have $R_e(\tilde{\sigma}) = O(\kappa'^2)$.

To check the above analysis, we present numerical results for case I from the full equation (25). Figure 2 shows plots of $Re(\tilde{\sigma})$ against κ' for parameter values of *C. nivalis* (see table 2), the different curves corresponding to different values of μ, the cosine of the angle the wavenumber vector makes with the z-axis. As μ increases, both the critical value of κ' and the maximum growth rate decrease; for $\mu = 1$ and $\kappa' > 0$, all roots of (25) have negative real part. There are no surprises here: the gyrotactic instability occurs for sufficiently small values of κ'. Quantitatively, too, the estimates based on (37) are pretty good for *C. nivalis*: the values of the critical value of κ' given by (38) are compared with the exact solution (from (25)) in table 4. We see excellent agreement for μ close to 0, getting worse as μ increases. In dimensional terms, the wavelength of the most unstable disturbance (with $\kappa' = 0.12$) is around 1.1 cm, not far from the spacing of streaks in the photograph in figure 2 of Pedley & Kessler (1992).

4.2. *Case II ($\lambda \ll 1$)*

In this limit we know that $\widehat{D}_V = 1$ and $\widehat{V} = K_1 - (V_S/V_O) \approx (\lambda/3) - (V_S/V_O)$. Now we also know that $V_S \ll V_0$ so, arbitrarily, we let $V_S/V_0 = \lambda(1/3 - q)$ so $\widehat{V} = \lambda q$ (q may have either sign). When numerical values are required we take $\widehat{D}_R = 1/6$ and $\alpha_0 = 0$

μ	κ_c' from (25)	κ_c' from (38)
0	0.439	0.439
0.2	0.434	0.431
0.5	0.404	0.386
0.6	0.384	0.360
$1/\sqrt{2}$	0.352	0.317
0.9	0.238	0.198
1	0	0

TABLE 4. Critical values of κ', below which *C. nivalis* is predicted to experience gyrotactic instability.

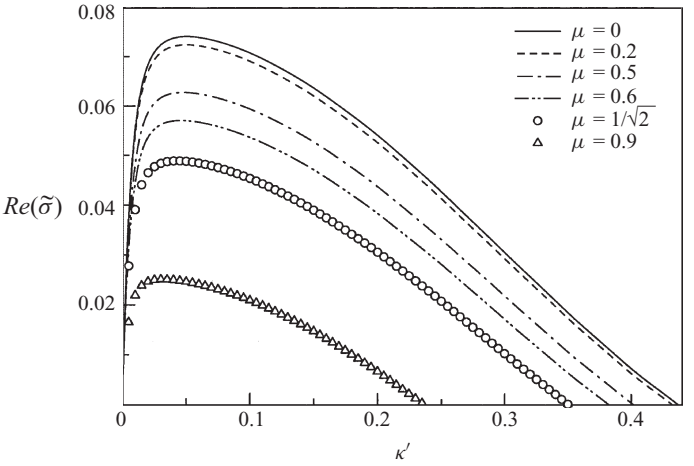

FIGURE 2. Growth rate as a function of wavenumber for case I, with parameters for *C. nivalis*. Different curves correspond to different values of $\mu = m/\kappa$, the cosine of the angle between the wavenumber vector and the vertical.

(spheres) or 1 (rods); the results will be qualitatively the same for all non-zero α_0. We recall that all quantities are calculated to $O(\lambda)$.

Twist. The equation for the growth rate is now (34), a quadratic equation, in place of (23), a linear one. Looking at (33), we see that the stresslet term involving $\widehat{S}$ has a simpler coefficient, but there is the factor $(\tilde{\sigma} + 6\widehat{D}_R)^{-1,}$ representing the non-quasi-steady nature of the p.d.f. $f(\boldsymbol{e})$ and hence of the perturbation to $\langle \boldsymbol{ee} \rangle^{(1)}$ in (17). Taking $\widehat{D}_R = 1/6$, the quadratic equation becomes

$$\tilde{\sigma}^2 + \tilde{\sigma}(\widehat{\nu}\kappa'^2 + 1 - \mathrm{i}\lambda q \kappa' \mu) + \kappa'^2\left(\widehat{\nu} + \frac{\alpha_0 \widehat{S}}{5}\right) - \mathrm{i}\lambda q \kappa' \mu = 0. \tag{44}$$

Thus, if $q = 0$, there is instability if and only if

$$\alpha_0 \widehat{S} < -5\widehat{\nu}\ ; \tag{45}$$

this is equivalent to (36), except that $J_2 = 0$, so instability requires $\alpha_0 \neq 0$ and $\widehat{S}$ negative and sufficiently large: rod-like pushers can drive a twist instability at any angle (the result is independent of μ). If $q \neq 0$, the same result holds even at very small κ'.

Splay. The equation for $\widetilde{\sigma}$ is now (35). Apart from being fourth order, because of the non-quasi-steadiness of $\langle \boldsymbol{ee} \rangle^{(1)}$, the main difference from (25) is the fact that $K_3 = 0$ to $O(\lambda)$ so the final stresslet term in (25) is absent. Hence, the SR instability given by (39) is also absent.

If gravity is negligible, because $\lambda\widehat{g}$ is very small, then (35) has two negative roots, and two which are the roots of (44), so splay modes are unstable under the same conditions as twist modes. When gravity is not negligible, we consider small κ' such that $\widehat{\nu}\kappa'^2$ and $\widehat{S}\kappa'^2$ are $O(1)$ (the Stokes limit). If $\alpha_0 = 0$, the stresslet term disappears altogether, so we take $\alpha_0 = 1$. If $\widehat{D}_R = 1/6$ (as is appropriate for small λ), (35) becomes

$$\widetilde{\sigma}^4 + \widetilde{\sigma}^3(4/3 + \widehat{\nu}\kappa'^2 - \mathrm{i}\lambda q\kappa'\mu) + \widetilde{\sigma}^2\left[\frac{1}{3} + \frac{1}{3}\left(\widehat{\nu} + \frac{3\widehat{S}}{5}\right)\kappa'^2 - \frac{4}{3}\mathrm{i}\lambda q\kappa'\mu\right]$$
$$+ \widetilde{\sigma}\left[\frac{1}{3}\left(\widehat{\nu} + \frac{\widehat{S}}{5}\right)\kappa'^2 - \frac{\lambda\widehat{g}\kappa'^2}{15}(1-\mu^2) - \frac{1}{3}\mathrm{i}\lambda q\kappa'\mu\right]$$
$$+ \frac{1}{3}\kappa'^4\left(\widehat{\nu} + \frac{\widehat{S}}{5}\right) - \frac{\lambda\widehat{g}\kappa'^2}{10}(1-\mu^2) - \frac{1}{3}\mathrm{i}\lambda q\kappa'^3\mu = 0. \tag{46}$$

If $\lambda q = 0$ and $\lambda\widehat{g} = O(1)$, then the second term in the coefficient of $\widetilde{\sigma}$ is negligible, and three of the roots of (46) are $O(1)$ and the same as those just discussed for zero $\lambda\widehat{g}$. However, the fourth root is $O(\kappa'^2)$ and is

$$\widetilde{\sigma} \approx -\kappa'^2 + \frac{\lambda\widehat{g}(1-\mu^2)}{2(5\widehat{\nu} + \widehat{S})}, \tag{47}$$

which, when $\widehat{g} > 0$, is positive for sufficiently small κ' as long as $\widehat{S} > -5\widehat{\nu}$, the opposite of (45). This is the gyrotactic instability and shows that gravity causes instability for pullers (and for not very strong pushers) whenever $\lambda\widehat{g}$ is positive. On the other hand, when $\widehat{g} < 0$, instability to this mode can occur only when (45) is satisfied. Putting $\lambda q \neq 0$ will have only a small effect on these results.

If we take $\kappa' \ll 1$ with $\widehat{\nu}$, $\widehat{S}$, $\lambda\widehat{g}$ all $O(1)$, then the results change, with $\lambda q \neq 0$ or $= 0$. Two roots of (46) are $O(1)$ and negative ($\widetilde{\sigma} \approx -1$ or $-1/3$), but the other two are $O(\kappa')$, and in fact are very similar to those given by (42) for general λ. In particular, when $\widehat{g} = -G < 0$ and $\lambda q = 0$, but $\alpha_0 \neq 1$, we have

$$Re(\widetilde{\sigma}) \approx \frac{\kappa'^2}{2}\left[\lambda G(1-\mu^2)\frac{(3-\alpha_0)}{2} - \widehat{\nu} - 1 - \alpha_0\frac{\widehat{S}}{5}\right]. \tag{48}$$

Thus, head-heavy gravity is weakly destabilizing but pullers are more stable than pushers. Once more, of course, viscosity is likely to damp out this instability in practice.

5. Discussion

This paper mainly elucidates the effects of particle stress S, gravity $\overline{g}$ and rotational diffusivity D_R on the instability of a uniform suspension of swimming micro-organisms. The basic state whose instability is examined is uniform, and the cells swim on average in the same direction, either because gravity applies an external torque to bottom- (or head-) heavy cells so that they swim upwards ($\overline{g} > 0$) or

downwards ($\overline{g} < 0$) (with an equivalent effect for sedimenting cells of uniform density but non-uniform geometry), or because the cells are responding to an external signal such as light or a chemical gradient and exhibit phototaxis or chemotaxis, which is modelled arbitrarily as if it were equivalent to an external torque ($\beta > 0$). The torque counteracts the tendency to isotropy driven by rotary diffusion. Cells are taken to be denser than the medium in which they are swimming ($\overline{g} \neq 0$) or neutrally buoyant ($\overline{g} = 0$). The cells may be pullers ($S > 0$) or pushers ($S < 0$).

The previous analyses of PHK and PK were for the bottom-heavy algal cells, *C. nivalis*, for which $\overline{g} > 0$ and $S > 0$, although PHK's analysis was for $S = 0$. PK included rotational diffusivity as well as particle stresses, but assumed that the p.d.f. of swimming direction was quasi-steady. PHK also did not consider bend–twist modes, for which the growth rates are given by (23), but that did not matter because these modes all decay for $\overline{g} > 0$, $S \geqslant 0$. In considering the splay modes (25), this paper has confirmed that the gyrotactic instability of PHK is not qualitatively affected by the presence of particle stresses.

Other previous analyses of note are those of SR and SS, who focused on the effect of particle stresses by considering the neutrally buoyant case, $\overline{g} = \beta = 0$, $S \neq 0$, without rotational diffusion ($D_R = 0$). They showed that long-wavelength instability would arise for both pullers and pushers, and that a suspension of pushers would also be unstable to bend–twist modes. These findings are confirmed here, and these instabilities dominate for large enough $|\widehat{S}|$ and small enough $|\widehat{g}|$. All modes of instability occur in the limit of long wavelength (small κ'). However, the two terms in the perturbation to the particle stress tensor (11) are responsible for two different modes of splay instability. One stems from the non-zero particle stress in the basic state, multiplied by the fluctuation in cell number density n'; this mode, in which the small growth rate is proportional to κ'^2, arises in the Stokes limit, i.e. in the absence of fluid inertia, and would occur for arbitrarily large viscosity if not limited by rotational diffusivity (see (40)). Both pushers and pullers give instability in this case. The other mode stems from the perturbation to $\langle \boldsymbol{ee} \rangle$ (multiplied by n_o) whether it is quasi-steady or not, and also gives a growth rate proportional to κ'^2, but only for pushers and only if $|\widehat{S}|/\widehat{\nu}$ exceeds a critical value of $O(1)$ (see (43*a*)). Therefore, none of the instabilities except the gyrotactic instability will arise unless the particle stresses are strong enough to overcome viscosity and/or rotational diffusivity.

It is of interest to see whether this is the case for the parameter values corresponding to the experiments of Kessler (1986, 1989), given in tables 1 and 2. To see the splay instabilities in the absence of gravity, the ratio $|\widehat{S}|/\widehat{\nu}$, equal to $n_o|S|D_H/\rho\nu V_o^2$, would have to be greater than the expression given by (40), for the SR mode, or $1/\max|B_1|$, for the other mode (see (43*a*)). According to table 2, $|\widehat{S}|/\widehat{\nu}$ is equal to 0.0033 for the *C. nivalis* experiments and to 0.79 for the *B. subtilis* experiments. The right-hand side of (40) is 0.59 and (approximately) 5×10^9, respectively (from table 2 and Appendix B), so in neither case will the SR mode survive, even if n_o is increased by a factor of 100. The quantity $1/|B_1|$ has a minimum value of 16.7 and 2.4×10^3 in the two cases, so the other particle-stress-driven mode is also not unstable in either case. In particular, for the bacterial suspension to be unstable, the cell number density would have to increase by a factor of 2400/0.79, i.e. to about 3×10^{12} cells cm^{-3}, for either of these two instabilities to be seen. At such large cell concentrations, the instability is of course possible, which may be the source of the coherent structures seen by Dombrowski *et al.* (2004), as postulated by SS, among others. It has been estimated that, in these experiments, the volume fraction of *B. subtilis* cells was about 30 %

(R. E. Goldstein, personal communication, 2009). Given the estimate of cell volume given in table 1, this is equivalent to $n_o \approx 2 \times 10^{12}$ cells cm^{-3}, which is close to the present estimate for the critical value.

A critical volume fraction was also predicted by SK in their recent very detailed analysis, in which the particle stress was also taken to be quasi-steady. Instability was predicted for bacteria (*E. coli*) if, in the present notation,

$$n_o L^3 > \frac{52.6(D_R L/V_o)}{1 - 2.05(D_R L/V_o)},$$

where L is the total length of the cell. Taking $L = 10\,\mu\text{m}$ gives $n_o > 2.5 \times 10^{10}$ cells cm^{-3}, which is 100 times smaller than the present prediction. However, some of the parameter values estimated here could well be incorrect, so the quantitative accuracy of the predictions is probably limited.

The most novel result in this paper is the instability, highlighted by (43*b*), which shows that a suspension of head-heavy swimmers ($\widehat{g} = -G < 0$) can be unstable even in the absence of particle stresses, if

$$\frac{B_2 G}{4\widehat{D}_R^2} > \widehat{\nu} + 1. \tag{49}$$

(This result was obtained for purely horizontal disturbances, for which $\mu = 0$, but the instability extends for non-zero values of μ.) This instability was not found by PK and arises from the fact that $f(\boldsymbol{e}, \boldsymbol{x}, t)$ is not here treated as quasi-steady when it is used to calculate the perturbation to the cell swimming direction, $\langle \boldsymbol{e} \rangle^{(1)}$, that is needed in the perturbed cell conservation equation (21). This leads to the factor $(\tilde{\sigma} + 2\widehat{D}_R)$ in (25), a factor that was not present in the PK model. The disturbance propagates horizontally with (dimensional) speed $V_o(B_2 G/2\widehat{D}_R)^{1/2}$ and grows slowly with growth rate $\kappa^2 \sigma_2$, σ_2 being given by (43*b*).

The physical mechanism of this instability can be understood from a simplified model in which particle stresses are absent ($S = 0$), cells are assumed to be spherical ($\alpha_o = 0$) and only horizontal disturbances are considered. We also neglect translational diffusion and viscosity (for now), though not fluid inertia. We assume a disturbance only in the x-direction, so that the leading contributions to the three governing (dimensionless) equations are as follows:

Vertical momentum (20*c*):

$$\frac{\partial w}{\partial t} = G n'. \tag{50}$$

Equation for perturbation to the average swimming direction (13):

$$\left(\frac{\partial}{\partial t} + 2D_R\right) e_{1x} = B_2 \omega_2 = -B_2 \frac{\partial w}{\partial x}. \tag{51}$$

Cell conservation equation (21):

$$\frac{\partial n'}{\partial t} = -\nabla \cdot \boldsymbol{e}_1 = -\frac{\partial e_{1x}}{\partial x}. \tag{52}$$

We recall that $\overline{g} = -G < 0$ and z (and w) are positive downwards. These equations can be combined into a single partial differential equation for w:

$$c^2 \frac{\partial^2 w}{\partial x^2} = \left(\frac{1}{2\widehat{D}_R}\frac{\partial}{\partial t} + 1\right)\frac{\partial^2 w}{\partial t^2}, \tag{53}$$

where $c^2 = B_2 G/2\widehat{D}_R$. Hence, in the absence of the $\partial/\partial t$ term in (51), this is the wave equation with wave speed c. When the $\partial/\partial t$ term is there, however, the amplitude of the wave grows with time, with growth rate $c^2/4\widehat{D}_R$, as found above, brought about by the delay in equilibration of the p.d.f. Of course, for realistic parameter values (49) shows that viscosity will suppress this instability unless n_o is extremely large (since G is proportional to n_o).

As noted in § 2, there are some *ad hoc* assumptions in the present model, mainly associated with (*a*) the translational and rotational diffusivities, and (*b*) the closure of the system of equations for the moments of the orientation distribution function f.

(*a*) We have first assumed that, in the cell conservation equation (6), random swimming can indeed be represented by a diffusivity tensor, equivalent to assuming that the cells' trajectories are Markovian random walks. Then, we have assumed that the randomness of these trajectories comes about from two sources: intrinsic differences between individuals within the population and rotational diffusion due to fluctuations in an individual's swimming mechanism. When rotational diffusion dominates, the translational diffusivity can be evaluated in terms of the rotational diffusivity as seen in (8) and demonstrated in Appendix A; this is the condition corresponding to small values of λ, and has been applied to head-heavy pushers (bacteria and spermatozoa) in the above discussion. However, for the larger algal cells, the estimated translational diffusivity (from PHK) and the estimated value of λ (from PK) are inconsistent with (8); we must assume that processes other than rotational diffusion are important.

(*b*) We have shown that the main gyrotactic and particle-stress-driven instabilities are not qualitatively affected by the assumptions used to close the sequence of moment equations such as (15) and (17). If $f(\boldsymbol{e})$ is taken to be quasi-steady, then the PK and SR models are appropriate (for zero S and zero $\overline{g}$ respectively). In particular, the SR instability arises in the Stokes limit, however large $\widehat{\nu}$ is. However, if $\langle \boldsymbol{e} \rangle$ is not quasi-steady, but $\langle \boldsymbol{ee} \rangle$ is, then two new features arise. One is that the magnitude of $\widehat{D}_R$ determines the critical value of $\widehat{S}/\widehat{\nu}$ (and hence n_o) for particle-stress-driven instability to take place (see (40)). The other is the new possibility of a wave-like instability for head-heavy cells, if the right-hand side of (43*b*) is positive. If $\langle \boldsymbol{ee} \rangle$ is also not quasi-steady, no new instability appears to arise, but this case has been investigated only in the small-λ limit. We should recognize that truncating the moment equations by assuming quasi-steady higher moments is strictly valid only for large $\widehat{D}_R$, but for a given $\widehat{D}_R$ the approximation gets better as the order increases: (15) for $\langle \boldsymbol{e} \rangle^{(1)}$ contains the factor $(\sigma_1 + 2D_R)$, (17) for $\langle \boldsymbol{ee} \rangle^{(1)}$ contains $(\sigma_1 + 6D_R)$, and the multiplier of D_R will be correspondingly larger for higher moments.

5.1. *Applicability of 'flocking' models*

As stated in the introduction, the model of SR was derived from the 'flocking' models of Vicsek *et al.* (1995) and Toner & Tu (1998), as fully expounded by Toner *et al.* (2005). The main differences lie in the equations for the cells' mean orientation. In our model, based on the torque or angular momentum balance for the cells, together with rotational diffusivity, these are derived from the Fokker–Planck equation and take the form of (15), (17), etc. The Toner & Tu model uses instead an equation for the cell velocity $\boldsymbol{V}$, relative to a fixed frame of reference, which takes the following

form when the interaction with the fluid is ignored:

$$\frac{\partial \boldsymbol{V}}{\partial t} + \lambda_1(\boldsymbol{V}\cdot\nabla)\boldsymbol{V} + \lambda_2(\nabla\cdot\boldsymbol{V})\boldsymbol{V} + \lambda_3\nabla(|\boldsymbol{V}|^2) = \alpha'\boldsymbol{V} - \beta'|\boldsymbol{V}|^2\boldsymbol{V} - \nabla p + D\nabla^2\boldsymbol{V} + D_B\nabla(\nabla\cdot\boldsymbol{V}). \quad (54)$$

Here the terms on the left-hand side with coefficients λ_i represent all possible quadratic terms that are not ruled out by symmetry considerations, and are permitted because the system does not exhibit Galilean invariance (which would require $\lambda_1 = 1, \lambda_2 = \lambda_3 = 0$). The same is true for the D_B term on the right-hand side. The 'body-force' terms $\alpha'\boldsymbol{V} - \beta'|\boldsymbol{V}|^2\boldsymbol{V}$ are an *ad hoc* representation of the fact that there is an equilibrium state in which all cells swim in the same direction with speed $V_0 = (\alpha'/\beta')^{1/2}$. The quantity p is a 'particle pressure' whose effect is to keep the cells apart, at a certain volume fraction, n_0, on average:

$$p = \sum_{j=1}^{\infty} \rho_j (n - n_0)^j, \qquad \rho_1 > 0. \quad (55)$$

The term $D\nabla^2\boldsymbol{V}$ in (54) represents translational diffusion of $\boldsymbol{V}$ and hence of $\boldsymbol{e} = \boldsymbol{V}/|\boldsymbol{V}|$. Presumably, this is supposed to arise from a combination of rotational diffusion and the variations within a real population, but the rotational diffusion (at least) is not modelled rationally, because the other features of non-zero D_R, included here, are not considered.

When fluid flow $\boldsymbol{u}$ is accounted for, there will be an additional advective term $(\boldsymbol{u}\cdot\nabla)\boldsymbol{V}$ on the left-hand side of (54) and reorienting viscous terms

$$\tfrac{1}{2}\,\boldsymbol{\omega}\wedge\boldsymbol{V} + \gamma_2\,\boldsymbol{e}\cdot\boldsymbol{E}\cdot(\boldsymbol{I} - \boldsymbol{ee}),$$

on the right-hand side, as in (9). However, in the present context, the *ad hoc* body force terms would not be the most rational way to represent the cells' locomotion relative to the fluid. Moreover, the SR model does not include a restoring torque, as represented by the β-term in (9).

The longitudinal $\widehat{\boldsymbol{k}}$ component of (54) gives an equation for the perturbation in swimming speed V'. If this is taken to be quasi-steady (as assumed by SR), the linearized form of the equation gives

$$2\alpha' V' + \rho_1 \mathrm{i} m n' = 0. \quad (56)$$

The existence of a non-zero V' has a knock-on effect in (6) above (and hence (21) also). However, the deterministic way of representing the equation for $\boldsymbol{V}$ (54) is inconsistent with the Fokker–Planck approach used here. The linearized analysis can be followed through, and shows that both the perturbation to the swimming speed and the particle pressure are stabilizing influences.

I am most grateful to Ms D. Pihler-Puzovic, Dr T. Ishikawa and Dr J. T. Locsei (who, in particular, showed me the derivations in Appendix A) for their help in the preparation of this work. I would also like to record my warm appreciation of the great pleasure, and great fun, that I derived from working with Steve Davis when we were co-editors of *JFM* from 2000 to 2006.

Appendix A. Relation between translational and rotational diffusivities

Let $\psi(\boldsymbol{e}, \boldsymbol{x}, t) = nf$ be the number density of cells in probability and physical space as a function of time ($n(\boldsymbol{x}, t)$ and $f(\boldsymbol{e}, x, t)$ are defined in the text). Then ψ satisfies

$$\frac{\partial \psi}{\partial t} + \nabla_x \cdot \left\{ (\boldsymbol{u} + V_o \boldsymbol{e} - V_s \widehat{\boldsymbol{k}})\psi - \boldsymbol{D}_T \cdot \nabla_x \psi \right\} + \nabla_e \cdot (\dot{\boldsymbol{e}}\psi) = D_R \nabla_e^2 \psi, \tag{A 1}$$

where

$$\dot{\boldsymbol{e}} = \beta \left[\widehat{\boldsymbol{k}} - (\widehat{\boldsymbol{k}} \cdot \boldsymbol{e})\boldsymbol{e} \right] \psi + \frac{1}{2} \boldsymbol{\Omega}_\wedge \boldsymbol{e} \psi + \alpha_o \boldsymbol{e} \cdot \widehat{\boldsymbol{E}} \cdot (\boldsymbol{I} - \boldsymbol{ee})\psi, \tag{A 2}$$

and $\boldsymbol{D}_T$ is a translational diffusivity, modelling all randomness except that due to random rotations. Integrating (A 1) over $\boldsymbol{e}$-space gives (6), in which

$$\boldsymbol{V} = V_o \langle \boldsymbol{e} \rangle = \frac{V_o}{n} \int \boldsymbol{e} \psi \, \mathrm{d}^2 \boldsymbol{e},$$

and $\boldsymbol{D}_T$ has been taken to be diagonal. If we multiply (A 1) by $V_o \boldsymbol{e}$ and integrate, we obtain the following equation for $\boldsymbol{V}$:

$$\frac{\partial}{\partial t}(n\boldsymbol{V}) + \nabla_x \cdot \left\{ (\boldsymbol{u} - V_s \widehat{\boldsymbol{k}}) n\boldsymbol{V} - \boldsymbol{D}_T \cdot \nabla_x (n\boldsymbol{V}) \right\} + V_o^2 \nabla_x \cdot (n \langle \boldsymbol{ee} \rangle) = V_o n \langle \dot{\boldsymbol{e}} \rangle - 2D^R n \boldsymbol{V}. \tag{A 3}$$

The manipulation leading to the last term is outlined below. Now, if the orientation distribution is dominated by rotational diffusion, and is therefore nearly quasi-steady and quasi-uniform, the top line of (A 3) may be neglected. It follows then that

$$V_o^2 \nabla_x \cdot (n \langle \boldsymbol{ee} \rangle) \approx V_o n \langle \dot{\boldsymbol{e}} \rangle - 2D_R n \boldsymbol{V}.$$

If it is additionally assumed that $V_o |\langle \dot{\boldsymbol{e}} \rangle| \ll D_R |\boldsymbol{V}|$, as for a small perturbation from an equilibrium distribution, then

$$n\boldsymbol{V} \approx -\frac{V_o^2}{2D_R} \nabla_x \cdot (n \langle \boldsymbol{ee} \rangle) \approx -\frac{V_o^2}{6D_R} \nabla_x n, \tag{A 4}$$

because in these circumstances the orientation distribution will be close to isotropic. Finally, substituting (A 4) into (6), we see that

$$-\nabla_x \cdot (n\boldsymbol{V}) \approx \frac{V_o^2}{6D_R} \nabla_x^2 n,$$

showing that rotational diffusion leads to an isotropic translational diffusivity of magnitude $V_o^2/6D_R$, i.e. (8). However, this result is dependent on the time scale for macroscopic variations of ψ being much larger than D_R^{-1}, so it will be valid for small growth rate and small wavenumnber in the stability problem of this paper.

A.1. *Manipulations in* $\boldsymbol{e}$*-space*

In integrating (A 1), multiplied by $\boldsymbol{e}$ or $\boldsymbol{ee}$, it is necessary to note that

$$\nabla_{ei} = (\delta_{ij} - e_i e_j) \frac{\partial}{\partial e_j}. \tag{A 5}$$

It follows that, for any function f,

$$\nabla_e^2 f = (\delta_{jk} - e_j e_k) \frac{\partial^2 f}{\partial e_j \partial e_k} - 2e_k \frac{\partial f}{\partial e_k}. \tag{A 6}$$

Integrals over $\boldsymbol{e}$-space (the unit sphere) involving derivatives are converted where possible to surface integrals using the divergence theorem, and the surface integrals are, in general, zero. Hence, for example,

$$\int \boldsymbol{e}\nabla_e^2 f \,\mathrm{d}^2\boldsymbol{e} = \int [\nabla_e \cdot (\boldsymbol{e}\nabla_e f) - \nabla_e \cdot \boldsymbol{e}\nabla_e f]\,\mathrm{d}^2\boldsymbol{e}$$
$$= + \int \nabla_e^2 \boldsymbol{e} f \,\mathrm{d}^2\boldsymbol{e} = -2\int \boldsymbol{e} f \,\mathrm{d}^2\boldsymbol{e} = -2\langle \boldsymbol{e}\rangle, \tag{A 7}$$

when $f(\boldsymbol{e})$ is the p.d.f. for $\boldsymbol{e}$, using (A 1) and (A 2). Similarly,

$$\int \boldsymbol{e}\boldsymbol{e}\nabla_e^2 f \,\mathrm{d}^2\boldsymbol{e} = 2\,[\boldsymbol{I} - 3\langle \boldsymbol{e}\boldsymbol{e}\rangle]\,. \tag{A 8}$$

Also

$$\int \boldsymbol{e}\nabla_e \cdot (\boldsymbol{B} f)\mathrm{d}^2\boldsymbol{e} = -\langle \boldsymbol{B}\rangle + \langle \boldsymbol{e}\boldsymbol{e}\cdot\boldsymbol{B}\rangle\,, \tag{A 9}$$

for any vector $\boldsymbol{B}$, and

$$\int \boldsymbol{e}\boldsymbol{e}\nabla_e \cdot (\boldsymbol{B} f)\mathrm{d}^2\boldsymbol{e} = -\langle \boldsymbol{B}\boldsymbol{e} + \boldsymbol{e}\boldsymbol{B}\rangle + 2\langle \boldsymbol{e}\boldsymbol{e}\,\boldsymbol{e}\cdot\boldsymbol{B}\rangle\,. \tag{A 10}$$

From these relationships, (A 3), (14) and (16) can be deduced.

Appendix B. Values of $B_1(\mu)$ and $B_2(\mu)$

The functions $B_1(\mu)$ and $B_2(\mu)$ are given by (26a) and (26b). For *C. nivalis,* with $\lambda = 2.2$, the values in tables 1–3 give

$$B_1 = 0.080(1-2\mu^2) - 0.020(1-2\mu^2)^2 - 0.092\mu^2(1-\mu^2),$$
$$B_2 = 0.224 + 0.020\mu^2,$$

so B_2 is positive for all μ, and B_1 may be either positive or negative. For all the pushers, for which $|\lambda|$ is very small, we have

$$B_1 \approx \frac{\lambda^3}{36}(1-2\mu^2) - \frac{\alpha_0\lambda}{15}\left[(1-2\mu^2)^2 + 9\mu^2(1-\mu^2)\right],$$
$$B_2 \approx \lambda\left\{\frac{1}{6} - \frac{\alpha_0}{10}\left[1 - \frac{\widehat{\beta}}{3}(1-2\mu^2(1-\alpha_0))\right]\right\}.$$

Hence, for small λ, $B_1 < 0$ unless $\alpha = 0$ and $\mu^2 < 1/2$; $B_2 > 0$ unless $\mu^2 > 1/(2(1-\alpha_0))$ (i.e. $\alpha_0 < 0.5$) and $\widehat{\beta}$ is large.

REFERENCES

Baskaran, A. & Marchetti, M. C. 2009 Statistical mechanics and hydrodynamics of bacterial suspensions. *Proc. Natl Acad. Sci.* **106**, 15567–15572.

Brenner, H. 1972 Suspension rheology. *Prog. Heat Mass Transfer* **5**, 89–129.

Bretherton, F. P. & Rothschild, Lord 1961 Rheotaxis of spermatozoa. *Proc. R. Soc. Lond.* **B153**, 490–502.

Childress, S., Levandowsky, M. & Spiegel, E. A. 1975 Pattern formation in a suspension of swimming micro-organisms. *J. Fluid Mech.* **69**, 591–613.

Dombrowski, C., Cisneros, L., Chatkaew, S., Goldstein, R. E. & Kessler, J. O. 2004 Self-concentration and large-scale coherence in bacterial dynamics. *Phys. Rev. Lett.* **93**, 098103.

Hillesdon, A. J. & Pedley, T. J. 1996 Bioconvection in suspensions of oxytactic bacteria: linear theory. *J. Fluid Mech.* **324**, 223–259.

Hillesdon, A. J., Pedley, T. J. & Kessler, J. O. 1995 The development of concentration gradients in a suspension of chemotactic bacteria. *Bull. Math. Biol.* **57**, 299–344.

Hinch, E. J. & Leal, L. G. 1972 The effect of Brownian motion on the rheological properties of a suspension of non-spherical particles. *J. Fluid Mech.* **52**, 683–712.

Katz, D. F. & Pedrotti, L. 1977 Geotaxis by motile spermatozoa: hydrodynamic reorientation. *J. Theor. Biol.* **67**, 723–732.

Kessler, J. O 1984 Gyrotactic buoyant convection and spontaneous pattern formation in algal cell cultures. In *Non-Equilibrium Cooperative Phenomena in Physics and Related Fields* (ed. M. G. Verlarde), pp. 241–248. Plenum.

Kessler, J. O 1985 Hydrodynamics focusing of motile algal cells. *Nature* **315**, 218–220.

Kessler, J. O. 1986 Individual and collective dynamics of swimming cells. *J. Fluid Mech.* **173**, 191–205.

Kessler, J. O. 1989 Path and pattern: the mutual dynamics of swimming cells and their environment. *Comments Theor. Biol.* **1**, 85–108.

Kessler, J. O., Hoelzer, M. A., Pedley, T. J. & Hill, N. A. 1994 Functional patterns of swimming bacteria. In *Mechanics and Physiology of Animal Swimming* (ed. L. Maddock, Q. Bone & J. M. V. Rayner), pp. 3–12. Cambridge University Press.

Mendelson, N. H., Bourque, A., Wilkening, K., Anderson, K. R. & Watkins, J. C. 1999 Organized cell swimming motions in *Bacillus subtilis* colonies: patterns of short-lived whirls and jets. *J. Bacteriol.* **181**, 600–609.

Pedley, T. J., Hill, N. A. & Kessler, J. O. 1988 The growth of bioconvection patterns in a uniform suspension of gyrotactic micro-organisms. *J. Fluid Mech.* **195**, 223–237.

Pedley, T. J. & Kessler, J. O. 1990 A new continuum model for suspensions of gyrotactic micro-organisms. *J. Fluid Mech.* **212**, 155–182.

Pedley, T. J. & Kessler, J. O. 1992 Hydrodynamic phenomena in suspensions of swimming micro-organisms. *Annu. Rev. Fluid Mech.* **24**, 313–358.

Roberts, A. M. & Deacon, F. M. 2002 Gravitaxis in motile micro-organisms: the role of fore–aft body asymmetry. *J. Fluid Mech.* **452**, 405–423.

Saintillan, D. & Shelley, M. J. 2008 Instabilities, pattern formation, and mixing in active suspensions. *Phys. Fluids* **20**, 123304.

Simha, R. A. & Ramaswamy, S. 2002 Hydrodynamic fluctuations and instabilities in ordered suspensions of self-propelled particles. *Phys. Rev. Lett.* **89**, 058101.

Subramanian, G. & Koch, D. L. 2009 Critical bacterial concentration for the onset of collective swimming. *J. Fluid Mech.* **632**, 359–400.

Toner, J. & Tu, Y. 1998 Flocks, herds and schools: a quantitative theory of flocking. *Phys. Rev.* E **58**, 4828–4858.

Toner, J., Tu, Y. & Ramaswamy, S. 2005 Hydrodynamics and phases of flocks. *Ann. Phys.* **318**, 170–244.

Vicsek, T., Czirok, A., Ben-Jacob, E., Cohen, I. & Shochet, O. 1995 Novel type of phase transition in a system of self-driven particles. *Phys. Rev. Lett.* **75**, 1226–1229.